World Applied Sciences Journal 3 (4): 577-589, 2008
ISSN 1818-4952

Determination of Sliding Path in Rock Slopes Containing Coplanar Non-Persistent Open Discontinuity

[1]A. Ghazvinian, [2]M.R. Nikudel and [1]V. Sarfarazi

[1]Rock Mechanics Division, University of Tarbiat, Modares, Tehran, Iran
[2]Department of Geology, University of Tarbiat, Modares, Tehran, Iran

Abstract: In 3-D analyses of rock slopes there're can be numerous sliding paths a long a coplanar non-persistent discontinuity with a known strike. This paper describes an approach for the determination of a most probable sliding path. For this particular study, several blocks of gypsum with the dimensions of 15×15×15 cm containing coplanar non-persistent open joints were fabricated. The models have various configurations of rock bridges occupying 45, 90 and 135 cm^2 of total shear surface (225cm^2) respectively. In order to study the complete failure behavior in the discontinuous joint, from each model, two similar blocks were prepared and were subjected to shear tests under two different normal stresses of 3.33 kg cm^{-2} and 7.77 kg cm^{-2}. The failure mechanisms were monitored by visual inspection and a low power microscope to detect crack initiation and propagation. For each test, the failure surfaces were investigated to determine the characteristics of each surface. Two types of newborn cracks were observed: wing (tensile) cracks and secondary (shear) cracks. Both types of cracks initiate from the tips of the joints and propagate in a stable manner. Based on the change in the configuration of rock-bridges, a factor called the Effective Joint Coefficient (EJC) was formulated, that is the ratio of the effective joint surface that is in front of the rock-bridge and the total shear surface. In general, the failure pattern is mostly influenced by the EJC while shear strength is closely related to the failure pattern and its failure mechanism. It is observed that the propagation of wing cracks or shear cracks depends on the EJC and the connection of wing cracks or shear cracks dominates the eventual failure pattern and determines the peak shear load of the rock specimens. So the EJC is a key factor in determination of sliding path.

Key word: Coplanar non-persistent discontinuity . rock bridge . Effective Joint Coefficient (EJC) . tensile and shear cracks

INTRODUCTION

One of the most important discussions in the rock mechanic engineering, is the investigation of stability of rock slopes and determination of their sliding path. In general, the stability of the rock slopes is related to factors such as slope height, topographical dip, discontinuity plane angle, the rock mechanical and physical properties, the tectonic status, the engineering properties of the rock joints, the overburden weight, presence of water and the effect of the earthquake or other acting forces. The determination of sliding path is important in rock slope stability analysis. In fact, with the prediction of the direction of the slide, it is possible to engineer a solution for the construction of the artificial structures around the rock slopes.

In 3-D analysis of rock slope stability, the engineering characteristics of the weak plane play an important role in the determination of the direction of the slide. Terzaghi [1], Robertson [2], Einstein *et al*. [3] suggest that the persistence of key discontinuity sets are in reality more limited and a complex interaction is needed in between the existing natural discontinuities and brittle fracture propagation through intact rock bridges to bring the slope to failure. So, besides the discontinuities themselves, the rock bridges, are of utmost importance for the shear strength of the compound failure plane [4, 5].

Different procedures can be used to study the strength of rock masses with non-persistent joints such as; field observations (as in the Hoek and Brown failure criterion); analytical solutions (as in Jenning's criterion); numerical studies (using available commercial software), or laboratory tests. Laboratory tests are an attractive procedure because they can expose failure mechanisms that may be complicated by other means. Laboratory tests are also useful to calibrate analytical solutions and numerical studies. Some previous results obtained with different test arrangements are summarized in the following paragraphs. Lajtai [6] performed direct shear

Corresponding Author: Dr. A. Ghazvinian, Rock Mechanics Division, University of Tarbiat, Modares, Tehran, Iran

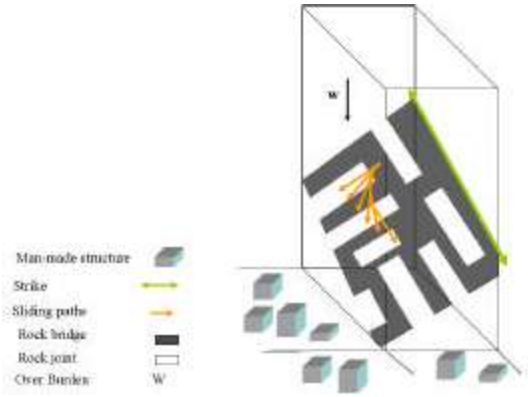

Fig. 1: The rock slope containing coplanar non-persistent open discontinuities

tests on model material with non-persistent joints and observed that the failure mode changed with increasing normal stress; he suggested a composite failure envelope to describe the transition from the tensile strength of the intact material to the residual strength of the discontinuities. He thus recognized that maximum shear strength develops only if the strength of the solid material and the joints are mobilized simultaneously. Other investigators conducted further experimental research to understand, in a qualitative way, the beginning, propagation and coalescence phenomena between two and three joints [7-17]. Gehle & Kutter's (18) investigation on the breakage and shear behavior of intermittent rock joints under direct shear loading condition showed that joint orientation is an important influential parameter for shear strength of jointed rock. Ghazvinian *et al*. [19] made a thorough analysis of the shear behavior of the rock-bridges based on the change in the persistence of their area. The analysis proved/showed that the failure mode and mechanism are under the effect of the continuity of the rock-bridge.

After surveying the various view points, it became obvious that the rock-bridges have an important effect on the design of the large rock slopes. In general, there are various paths exist for sliding of a coplanar open non-persistent rock joint having a characteristic strike (Fig. 1).

Under these conditions, the aperture of the joints and their engineering characteristics do not affect the sliding path. It was assumed that the overburden weight W (normal stress) and the area of the rock-bridge have a uniform distribution in the entire possible slide paths, thus, have no effect in the determination of sliding path.

The configuration of the rock-bridges alone is the key factor in determination of the slide path, in case, the effects of dynamic, water and asymmetrical forces are not considered, In this paper, the effect of the configuration of the rock-bridges on the shear resistance of the open non-persistent rock joints (in the fixed area of the rock-bridge) is studied. By using this pilot study, the sliding path of the rock slopes described in Fig. 1 is determined.

EXPERIMENTAL STUDIES

The discussion of experimental studies is divided into four sections. The first section discusses the physical properties of a modeling material, the second section is describing the technique of preparing the jointed specimens, the third section is focused on the testing procedure in loading the jointed specimens and finally, the fourth section considers the general experimental observations and discussions.

Modeling material and its physical properties: Full scale testing on a rock mass containing a specified number of joints with predetermined configuration is seldom possible. The common procedure to the problem is to conduct experiments under conditions that are attainable, but the patterns of discontinuities involved in the prototype have to be preserved in the model experiments and the modeling material must behave similar to rock mass. The most comprehensive review on how to select a modeling material for rocks is probably by Stimpson [20]. Although there are a number of modeling materials that can be considered as rock-like [21-23].

The material used for this investigation is gypsum, the same material was used by Reyes and Einstein [7], Takeuchi [24], Shen *et al*. [25] and Bobet and Einstein [9]. Gypsum is chosen because, in addition to behave same as a weak rock, is an ideal model material with which a wide range of brittle rocks can be represented [26]; second, all the previous experiences and results can be incorporated and the earlier findings can be compared with the new ones; third, it allows to prepare a large number of specimens easily; Forth, repeatability of results.

The samples are prepared from a mixture of the water and gypsum with a ratio of water to gypsum = 0. 75.

Concurrent with the preparation of specimens and their testing, uniaxial compression and indirect tensile strengths of the intact material was also tested in order to control the variability of material. The uniaxial compressive strength (UCS) of the model material is measured on fabricated cylindrical specimens with 56 mm in diameter and 112 mm in length. The indirect tensile strength of the material is determined by the Brazilian test using fabricated solid discs 56 mm in diameter and 28 mm in thickness.

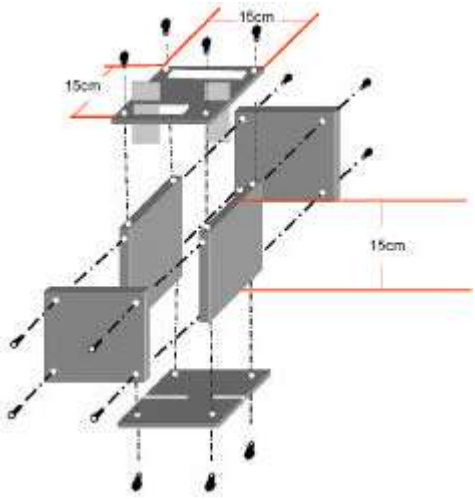

Fig. 2: Model used for the fabrication of the gypsum specimens

The testing procedure of uniaxial compressive strength test and the Brazilian test complies with the ASTM D2938-86 [27] and ASTM C496-71 [28], codes respectively. Four transducers were used to measure the horizontal and vertical displacements in universal USC Tests. Three of the transducers are set to touch the middle of the cylindrical specimen longitudinally along a diametrical line at 120 degrees to each other while the other one is set to touch the base of the lower platen.

The displacement transducers and load cell were connected to a data logger which was further linked to a PC for data recording. The base material properties derived from unconfined compression and tensile test are as follows:

Average uniaxial compressive strength:	37.5 MPa
Average brazilian tensile strength:	4 MPa
Average Young's Modulus in compression:	6020 MPa
Average Poisson's ratio:	0.18

The technique in preparing the jointed specimens: Jointed specimens may be prepared by different methods that in general can be classified into two categories. The first involves inserting a medium between the two opposing surfaces that provides a lower friction angle in relation to the friction angle of the solid rock (Stimpson [29]). The second method entails assembling individual small blocks in a specific shape to form a large mass containing persistent or non-persistent joints Brown and Trollope [30]; Rosenblad [31]; Ladanyi and Archambault [32]).

The formation of jointed rock masses from individual block elements has the following shortcomings: Imperfect matching; Imperfect closure; Imperfect matching or improper fitting of individual elements loads to concentration of stresses; Rotation; and Non-uniformity of the individual elements.

Due to the above-mentioned reasons Bobet [9] developed a new method to form blocks with non-persistent joints during casting. The procedure developed by Bobet [9] for preparing open non-persistent joints was used in this research with some modifications. Following is a description of the procedure of making open coplanar non-persistent joints with different configurations.

The material mixture is prepared by mixing water and gypsum in a blender; the mixture is then poured into a steel mold with internal dimension of 15×15×15 cm. The mold consist of four steel sheets, bolted together and of two PMMA plates 1/6 inch thick, which are placed at the top and bottom of the mold, as shown in Fig 2; the top plate has two rectangular openings used to fill the mold with the liquid gypsum mixture. The upper and the lower surfaces have slits cut into them. The opening of slits is 0.5 mm (0.02 inch) and their tract varies based on the width of the joints.

The positions, number and shape of the slots are predetermined to give a desired non-persistent joint. Through these slits, greased metallic shims are inserted through the thickness of the mold (to produce open joints) before pouring the gypsum. The mold with the fresh gypsum is vibrated and then stored at room temperature for 8 h afterward, the specimens un-molded and the metallic shims pulled out of the specimens; the grease on the shims prevents adhesion with the gypsum and facilitates the removal of the shims.

As the gypsum seated and hardened, each shim leaves in the specimen an open joint through the thickness and perpendicular to the front and back of the specimen. Immediately after removing the shims, the front and back faces of the specimens are polished and the specimen is stored in laboratory for 4 days. At the end of the curing process, the specimens are tested. It does not appear that the pull out of the shims produces any damage to the flaws. A number of pairs of PMMA plates are prepared with different slit arrangements to produce the desired joint geometries.

The coplanar rock bridges have various configurations respect to shear loading direction and have occupied 45, 90 and 135 cm^2 of the total shear surface (225 cm^2) respectively. The geometry of non-persistent joints has shown in Table 1. The Rock bridge dimensions is defined by two parameters a and d. The joint dimensions are defined by four parameters b, c, d and e.

Based on the change in the configuration and area of the rock-bridges, it is possible to define the Effective Joint Coefficient as the ratio of the effective joint surface (that is in front of the rock-bridge) and the total shear surface.

Table 1: The geometrical specifications of the various rock bridges

Rock Bridge Set	R.B Area (cm^2)	a	b	c	d	e
	45	3	6	-	15	-
	90	6	4.5	-	15	-
	135	9	3	-	15	-
	45	3	6	-	15	-
	90	6	4.5	-	15	-
	135	9	3	-	15	-
	45	5	5	-	9	6
	90	9	3	-	10	5
	135	10	2.5	-	13.5	1.5
	45	5	5	-	9	6
	90	9	3	-	10	5
	135	10	2.5	-	13.5	1.5
	45	1.5	4	4	15	-
	90	3	3	3	15	-
	135	4.5	2	2	15	-
	45	1.5	4	4	15	-
	90	3	3	3	15	-
	135	4.5	2	2	15	-
	45	2.5	4	2	9	6
	90	4.5	2	2	10	5
	135	5	2	1	13.5	1.5
	45	2.5	4	2	9	6
	90	4.5	2	2	10	5
	135	5	2	1	13.5	1.5

Rock Bridges
Joint

In Table 2, the effective surface of the non-persistent rock-joint is shown as surrounded area between the black dotted lines (in front of the rock bridges). Furthermore, the amount of the EJC is exhibited in this table.

In order to study the complete failure behavior in the discontinuous joint, from each geometry, two similar blocks were prepared and were tested under two different normal stresses (σ_n): 3.33 and 7.77 kg cm^{-2}.

Two identical specimens for each normal loading are prepared and tested to check repeatability. If the results from two identical tests show significant differences, a third specimen is prepared and tested.

Testing Equipment: Testing of the specimens is done in direct shear until failure. These tests have been performed in an especially designed shear machine which complies with the requirements that

Table 2: The amounts of the Effective non-persistent Joint Coefficients (EJC) for various configurations

Rock Bridge Set	R.B Area ($a \times d'$)	Effective Joint Surface (EJS)	Total Shear Surface (TSS)	Effective Joint coefficient (EJC= EJS/TSS)
A	a 45	0	225	0
	a' 90	0	225	0
	a'' 135	0	225	0
B	b 45	180	225	0.8
	b' 90	135	225	0.6
	b'' 135	90	225	0.4
C	c 45	30	225	0.13
	c' 90	45	225	0.2
	c'' 135	15	225	0.06
D	d 45	90	225	0.4
	d' 90	60	225	0.26
	d'' 135	67.5	225	0.3
E	e 45	0	225	0
	e' 90	0	225	0
	e'' 135	0	225	0
F	f 45	180	225	0.8
	f' 90	135	225	0.6
	f'' 135	90	225	0.4
G	g 45	30	225	0.13
	g' 90	45	225	0.2
	g'' 135	15	225	0.06
H	h 45	90	225	0.4
	h' 90	60	225	0.26
	h'' 135	67.5	225	0.3

were found to be indispensable in conventional shearing devices. Consequently, the shear boxes were provided with a high stiffness and with only one degree of freedom for the lower shear box in the horizontal direction and for the upper one in the vertical direction, corresponding to a shear displacement or dilation, respectively. Unwanted rotations and uncontrolled loading conditions could be prevented this way. The second main requirement comprised the possibility to permanently observe the cracking process in the sheared specimens. Therefore, the shape and arrangements of the shear boxes permitted free access to front and back sides of the specimens.

Testing program: A total of 96 direct shear tests have been performed on specimens with discontinuous joints. All tests are displacement-controlled. The tests were performed in such a way that the normal load was applied to the sample and then shear load was adopted. Readings of shear loads, as well as the shear displacements are taken every two seconds by a data acquisition system. During loading, the rock bridge surface is scanned with a low power microscope. A camera is attached to the microscope and connected to a TV monitor and VCR. An independent fiber optic illumination device lights the scanned surface. Figure 3 shows a schematic of the

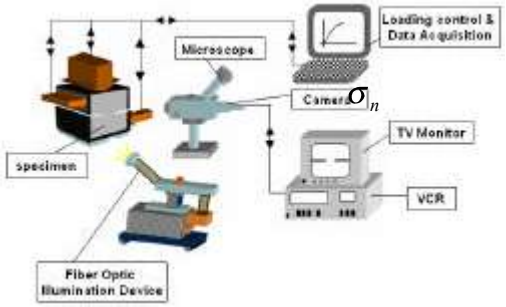

Fig. 3: Schematic of experimental set-up

scanning and the loading control systems. After the test is finished, the tape is viewed again and the images are digitized.

Loading is carried out using displacement control at a rate of the 0.002 mm/s. This rate is adopted because it facilitates the observation of crack initiation. After each step, loading is stopped, without un-loading, the rock bridge surface is scanned for new cracks. Once the scan is completed a new loading step is applied. This process is necessary to accommodate scanning.

The Joint slippage, crack pattern, coalescence type and coalescence stress, are the basic measurements and observation made during the testing. The crack pattern after failure is measured/observed after the test is completed and the specimen has been taken out of the machine. It was observed, during experiments, that the pre-existing joints remain open until the coalescence; immediately afterwards the joints close, at least partially. The shearing process of a discontinuous joint constellation begins, as one would expect, with the formation of new fractures which eventually transect the material bridges and lead to a through-going discontinuity.

OBSERVATION

By observing the failure surface during and after the tests, it is possible to investigate the effect of bridge configurations (or EJC) on the failure mechanism of specimens. Figures 4-6 summarizes all observed crack patterns obtained in the direct shear tests.

The crack pattern is always a combination of only two types of cracks: wing cracks and shear cracks. Wing cracks start at the tip of the joints and propagate in a curvilinear path as the load increases. Wing cracks are tensile cracks and they grow in a stable manner, since an increase in load is necessary to lengthen the cracks. Shear cracks also initiate at tip

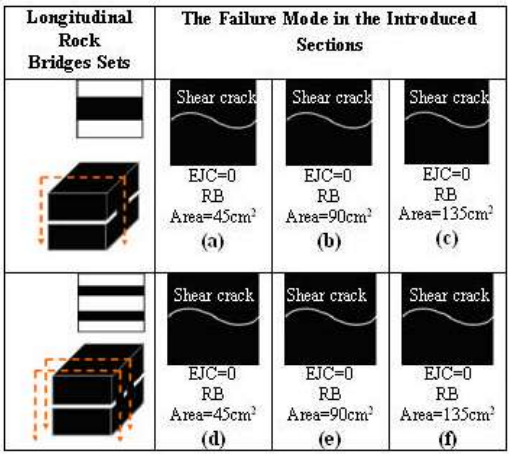

Fig. 4: The failure patterns in longitudinal rock bridges with EJC = 0

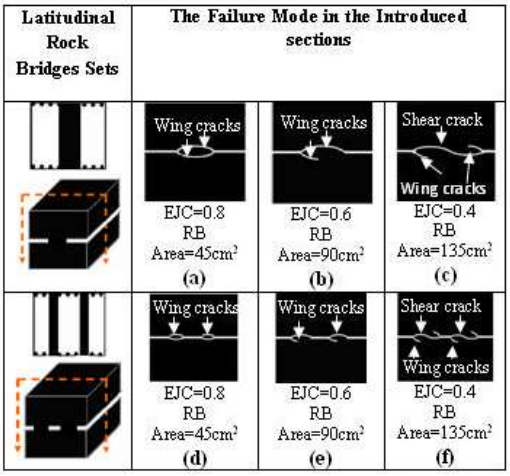

Fig. 5: The failure patterns in latitudinal rock bridge

of the joints or initiate at the edges of the samples and propagate in a stable manner.

Type I: The pure shear failure in persistent longitudinal rock bridges: The pure shear failure, as defined in Fig. 4, occurs when EJC=0; i.e. the persistent rock bridge have longitudinal configuration. In this case the shear cracks initiated at the tip of the rock-bridges that are at the edges of the sample (the r and r′ positions in Table 2A) and propagated to meet each other at a point in the bridge. Afterward the rock bridge gets broken into two parts from the middle with an uneven shear failure surface.

The characteristics of the failure surface were investigated. There was a significant amount of pulverized and crushed gypsum and traces of shear displacement, indicated that a shearing failure had taken place. The shear failure mode appears in all types of samples consisting longitudinal rock-bridges (Fig. 4).

Type II: The oval mode coalescence with two wing cracks in persistent latitudinal rock bridges: The oval mode coalescence, as defined in Fig. 5a and 5d, occurs when EJC=0.8; i.e. rock bridges have latitudinal configuration and theirs area is 45 cm^2. The wing cracks were initiated and propagated in curvilinear path that eventually aligned with the shear loading direction.

The wing cracks propagate in a stable manner; and the external load needs to be increased for the cracks to propagate further. Each wing crack was initiated at the tip of one joint and finally coalesced with the tip of the other joint.

This coalescence left an oval core of intact material completely separated from the sample (Fig. 5a and 5d). The surface of failure at the bridge area is tensile because no crushed or pulverized materials and no evidence of shear movement were noticed. The wing cracks surfaces also had the same characteristics of tension surface. It is to be note that, when EJC=0.8 the oval mode coalescence appeared in samples consisting one and two latitudinal rock bridges.

Type III: Coalescence with one wing crack in persistent latitudinal rock bridges: This coalescence, as defined in Fig. 5b and 5e, occurred when EJC=0.6; i.e. the persistent rock bridges have latitudinal configuration and theirs area is 90 cm^2. In this configuration the wing cracks were initiated at the tip of the joints and propagated stably. The upper tensile crack can propagate through the intact portion area and finally coalesced with the inner tip of the other joint but the lower tensile crack develops for a short distance and then become stable so as not to coalesce with the tip of opposite joint.

Examining the wing crack surface it was noticed that there was smooth and clean with no crushed or pulverized material and no evidence of shear displacement. These surface characteristics indicated that tensile stresses were responsible for the initiation and propagation of the wing cracks. It is to be note that, when EJC=0.6 this coalescence appears in samples consisting one and two latitudinal rock bridges.

Type IV-Coalescence with two shear cracks in persistent latitudinal rock bridges: Coalescence with shear cracks, as defined in Fig. 5c and 5f, occurs when EJC=0.4; i.e. the persistent rock bridges had latitudinal configuration and theirs area is 135 cm^2. The mechanism of failure was characterized first by initiation of wing cracks followed by the initiation of secondary cracks at the tips of the joint segments.

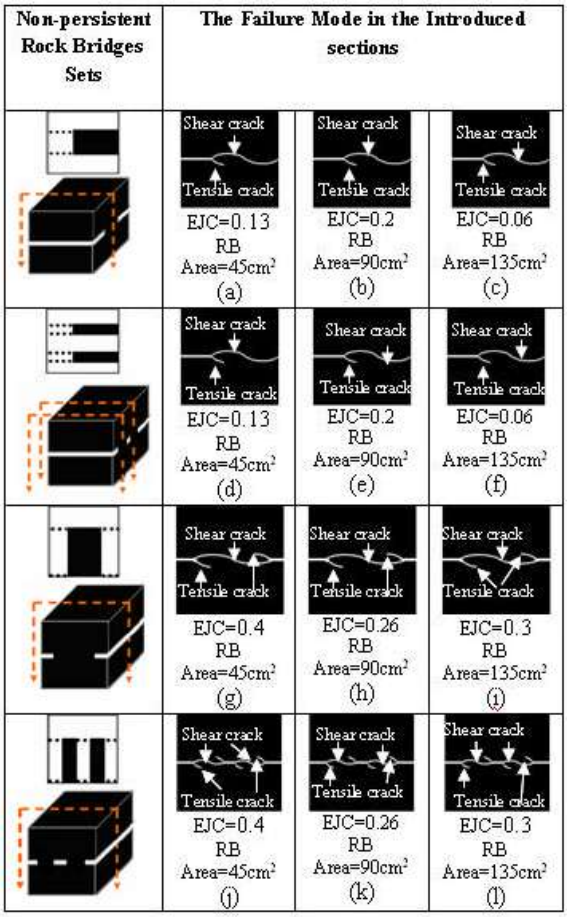

Fig. 6: The failure patterns in non-persistent rock bridges

Then the two wing cracks stopped while the two secondary cracks propagated to meet each other at a point in the bridge between the two inner tips of the preexisting joints. The propagation and coalescence of the secondary cracks brought rock bridges to failure. The shear failure surface is in a wavy mode. Inspection of the surface of the cracks producing coalescence reveals the presence of many small kink steps, crushed gypsum and gypsum powder, which suggested coalescence through shearing. It is to be note that, when EJC=0.4, this coalescence appears in samples consisting one and two latitudinal rock bridges.

As for the other experimental samples in this part, the failure patterns obtained from this experiment are in reasonable accordance with some of the related experimental results in Refs [6, 33].

Type V: Coalescence with one undulating shear crack in non-persistent longitudinal rock bridges: This type of coalescence, as defined in Fig. 6, occurs when longitudinal rock bridges are non-persistent and EJC<0.4 (Fig. 6a-f).

In this case, one wing crack was initiated at the inner tip of the joint and propagated stably in curvilinear path. Then the wing crack stopped while the secondary crack initiated at the inner tip of the joint and propagated stably to coalesce with the right edge of the sample, as shown in Fig. 6a-f. It is to be noted that, when EJC < 0.4 this coalescence appeared in samples consisting one and two longitudinal non-persistent rock bridges.

Type VI: Coalescence with two shear cracks in latitudinal non-persistent rock bridges: This type of coalescence, as defined in Fig. 6, occurs when latitudinal rock bridges are non-persistent and EJC<0.4 (Fig. 6g-l). In this case, two wing cracks were initiated at the tips of the joints and propagated in curvilinear path. Then the two wing cracks stopped while the two secondary cracks initiated at the tips of the joint segments and continued to join together at a point in the bridge. It is to be note that, when EJC < 0.4 this coalescence appears in samples consisting one and two latitudinal non-persistent rock bridges.

By examining the failure surface for non-persistent rock bridges, it was found that the shear failure surface is in a wavy mode. The traces of shear displacement existed and pulverized and crushed materials could be found. These surface characteristics indicated that shear stresses were responsible for the initiation of the shear cracks.

DESCRIPTION OF THE FAILURE MODES

The failure mode correlates quite well with the continuity of the joints and rock bridges, which can be described by the ''effective joint Coefficient''.

Type I: The pure shear failure in persistent longitudinal rock bridges (Fig. 4): When longitudinal rock bridges extend through the shear surface (i.e. they are persistent), EJC is equal to 0. It means that there isn't any joint surface in front of the rock-bridge tips (Table 2A and E). In this case, the stress concentration doesn't exist at any point in the shearing path. It can be assumed a uniform distribution of stress over the plane of the rock bridge.

When the external shear loading reaches a critical value, the shear crack initiation occurs at the edges of the specimen (r and r′ situations in Table 2A and E). The initial crack growth will propagate if the stress concentration induced by their growth be greater than the material shear strength existing in crack tips. Otherwise, the external shear loading must be increased.

We observed that the shear cracks propagate in a stable manner since an increase in external load is necessary to increase the shear stresses concentration at tips of the shear cracks. The shear stresses concentrations reach to critical value and lengthen the cracks and bring the rock bridges to failure (Fig. 4).

Case II: The oval mode coalescence with two wing cracks in persistent latitudinal rock bridges (Fig. 5a and d): For the persistent latitudinal rock-bridges with the EJC=0.8 (the area of the rock-bridges are 45 cm^2), there is very large extension of joint surface in front of the rock-bridge tips (Table 2Bb and Ff) and limited distance between the tip of the joints (r and r? in Table 2 Bb and Ff) is short. Therefore a very high stress concentration (tensile and shear) is established due to the interaction between the joint tips. The tensile strength of the material existing at the tip of the joints are less than the shear strength and tensile stress intensity at tips of the joints is strong enough to produce the small tensile cracks tending to split the rock bridge.

Since, the tensile stress intensity is not enough to cause unstable crack growth therefore an increase in external load is necessary to elongate the existing tensile cracks. After the wing crack has grown enough, the contribution of the wing opening to the stress field redistribution becomes significant. In this time, the crack-generated tensile stress field and the effect of interaction between the crack tip and opposite joint tip (that are indeed situated very close to each other) is so strong that tend to unstable wing cracks growth connecting the joints. Since no new fracture produces in the midst zone, the coalescence left an oval core of intact material completely separated from the sample (Fig. 5a and d).

Type III: Coalescence with one wing crack in persistent latitudinal rock bridges (Fig. 5b and e): For persistent latitudinal rock-bridges with the EJC=0.6 (Table 2 Bb? and Ff?), According to the characteristic of the failure surface, it seems that at first high tensile stresses concentration reaches to tensile strength of material existing at the tips of the joints and wing cracks initiate. The tensile strength of material is less than its shear strength so before the shear stresses concentration could overcome to shear strength, the tensile stress concentration reach to critical value and wing cracks initiate at tips of the joints. The lower wing crack stopped and the upper one propagated suggesting that the tensile stresses were eliminated at the lower wing crack and persisted at the upper wing crack. The upper crack growth propagates if the tensile stress concentration is enough.

With increasing external loading, the tensile stresses concentration reaches to critical value again and the upper tensile crack can propagate through the intact portion area

but the lower tensile crack develops for a short distance and then becomes stable so as not to coalesce with the tip of other joint (Fig. 5b and 5e).

Type IV: Coalescence with two shear cracks in persistent latitudinal rock bridges (Fig. 5c and f): For the persistent latitudinal rock-bridges with the EJC=0.4 (Table 2 Bb" and Ff"), a high stress concentration (tensile and shear stresses) is established at tips of the joints due to high external loading. At first, the tensile stresses reach to critical value (because the tensile strength of the material existing at the tip of the joints is less than its shear strength) and two wing cracks initiated at the tips of the joints.

The tensile stresses released due to wing cracks initiated at the tips of the joints so two wing cracks stopped. With increasing in external loading, the tensile stress concentration at tips of the wing cracks reach to critical value again and tensile cracks can propagate for a short distance in a curvilinear path. Before the wing cracks could propagate further, the shear stress concentration initiated secondary cracks at the tips of the preexisting joints.

The external shear loading must be increased that cause the shear stresses concentration at tips of the shear cracks overcome to shear strength of material existing in joint tips. This shear cracks propagate till the end of the test. The propagation and coalescence of the secondary cracks brought rock bridges to failure in a wavy mode (Fig. 5c and 5f).

Type V: Coalescence with one undulating shear crack in non-persistent longitudinal rock bridges (Fig. 6a-f): For longitudinal configuration of non-persistent rock bridge that EJC <0.4 (Table 2C and G) a high stress concentration (tensile and shear stresses) is established at tip of the joint. Initially, the wing crack was formed at tip of the joint due to reaching the tensile stress concentration to critical value. Before the wing crack could extend till the right edge of the specimen, the shear stress concentration initiated a secondary crack at the tip of the preexisting joint. The shear stress released due to shear crack initiated. Since an increase in external load is necessary to increase the stress concentration at tip of the cracks. Before the tensile stress concentration could overcome to tensile strength of material existing at tip of the wing crack, the shear stress concentration at tip of the shear crack reaches to critical value and shear crack propagate and coalesce with the right edge of the specimen in an undulating mode.

The shear failure mode appears in all types of samples consisting longitudinal non-persistent rock bridges (Fig. 6a-f).

Type VI: Coalescence with two shear cracks in latitudinal non-persistent rock bridges (Fig. 6g-l): For longitudinal configuration of non-persistent rock bridge with EJC<0.4 (Table 2D and H), a high stress concentration (tensile and shear stresses) is established at tips of the joints due to high external loading. At first the tensile stresses reach to critical value (because the tensile strength of the material existing at the tip of the joints is less than its shear strength) and two wing cracks initiated at the tips of the joints. The tensile stresses released due to wing cracks initiated at the tips of the joints so two wing cracks stopped. With increasing in external loading, the tensile stresses concentration at tips of the wing cracks reach to critical value again and tensile cracks can propagate for a short distance in a curvilinear path. Before the wing cracks could propagate further, the shear stresses concentration initiated secondary cracks at the tips of the preexisting joints. The shear stresses released due to shear cracks initiated. So the external shear loading must be increased that cause the shear stresses concentration at tips of the shear cracks overcome to shear strength of material existing in joint tips. This shear cracks propagate till the end of the test. The propagation and coalescence of the secondary cracks brought rock bridges to failure in a wavy mode. The shear failure mode appears in all types of samples consisting latitudinal non-persistent rock bridges (Fig. 6g-l).

THE EFFECT OF THE EFFECTIVE JOINT COEFFICIENT (EJC) ON THE RESISTANCE OF ROCK BRIDGE

Figure 7 and 8 shows the rock-bridge resistance versus the EJC for one and two rock-bridges, respectively. Each figure summarizes the resistance at failure for three values of rock-bridge areas (45 cm^2, 90 cm^2 and 135 cm^2). the upper line and the lower line in Each panel represents the resistance of rock bridge under two value of the normal stress of 3.33 and 7.77 kg cm^{-2} respectively. From the Fig. 7 and 8, it can be found that for the fixed area of the rock bridge under fixed normal stress, the resistance decreases dramatically by increasing the EJC. The rock bridge resistance is maximum and minimum for longitudinal and latitudinal fully persistent rock bridge respectively. In fact, the coalescence stress depends on the EJC affecting the type of coalescence. When the rock-bridge extends longitudinally over the shear surface (EJC=0), there isn't any joint surface in front of the rock-bridge tips (Table 2A and E).

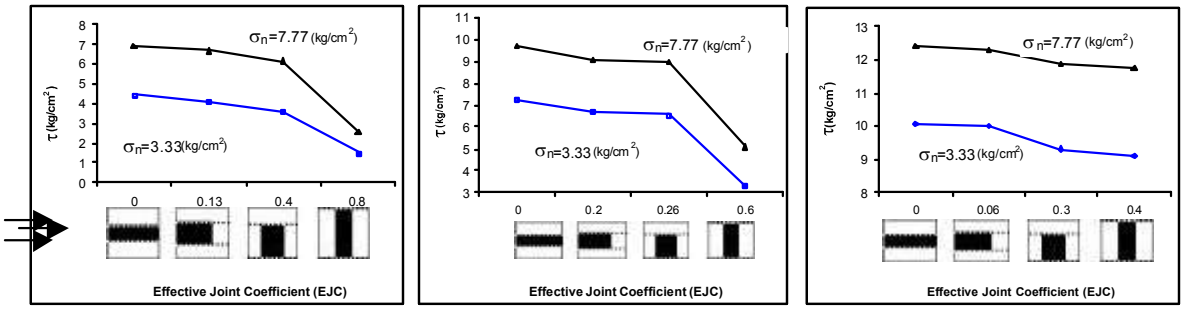

(a) (b) (c)

Fig. 7: Shear resistance versus effective joint coefficient (for one rock bridge); a: Area of the rock bridges is 45 cm^2, b: Area of the rock bridges is 90 cm^2, c: Area of the rock bridges is 135 cm^2

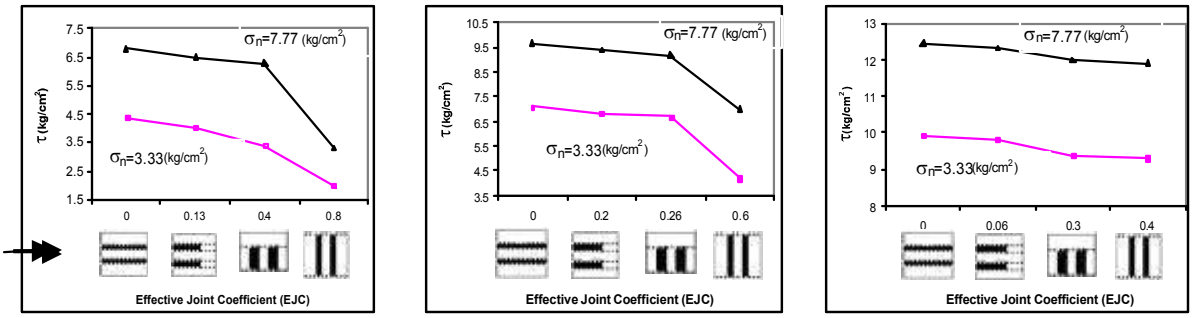

(a) (b) (c)

Fig. 8: Shear resistance versus effective joint coefficient (for two rock bridges); a: Area of the rock bridges is 45 cm^2, b: Area of the rock bridges is 90 cm^2, c: Area of the rock bridges is 135 cm^2

In this case, the stress concentration doesn't exist at the tip of the rock-bridge (r and r? situations at the right and left edges of specimen in Table 2A and 2E) and the rock-bridge fails in its final resistance so has the maximum resistance. From the Fig. 7 and 8, it can be found that for the fixed area of the rock bridge under fixed normal stress, the resistance decreases dramatically by increasing the EJC. The rock bridge resistance is maximum and minimum for longitudinal and latitudinal fully persistent rock bridge respectively. In fact, the coalescence stress depends on the EJC affecting the type of coalescence. When the rock-bridge extends longitudinally over the shear surface (EJC=0), there isn't any joint surface in front of the rock-bridge tips (Table 2A and E). In this case, the stress concentration doesn't exist at the tip of the rock-bridge (r and r? situations at the right and left edges of specimen in Table 2A and E) and the rock-bridge fails in its final resistance so has the maximum resistance. With the change in the configuration of the rock-bridge, the effective joint is formed in front of the rock-bridge, in such a way that in the latitudinal configuration of the rock-bridges, the value of EJC is maximum (Table 2B and F).

The more be EJC, the higher be stress concentration at tips of the joints. So the smaller external loading need for reaching the stress concentration at tip of the joints to critical value.

It means that the rock bridge resistance decreases by increasing the EJC. Since the longitudinal and latitudinal fully persistent rock-bridges have the minimum and maximum EJC, so their resistance behavior will be inspected in following section.

COMPARISON OF THE LATITUDINAL ROCK BRIDGE RESISTANCE IN THE VARIOUS AREAS OF THE ROCK BRIDGE

Figure 9 and 10 shows the rock-bridge resistance versus the area of one and two rock-bridges, respectively. Each figure summarizes the resistance at failure (τ_p) under two different values of normal stresses (σ_n) of 3.33 and 7.77 kg cm^{-2} respectively. The upper line and the lower line in each panel represent the resistance of longitudinal and latitudinal rock bridge respectively. By comparing the resistance of the longitudinal and latitudinal rock-bridges in each figure, it is possible to reach the following conclusions.

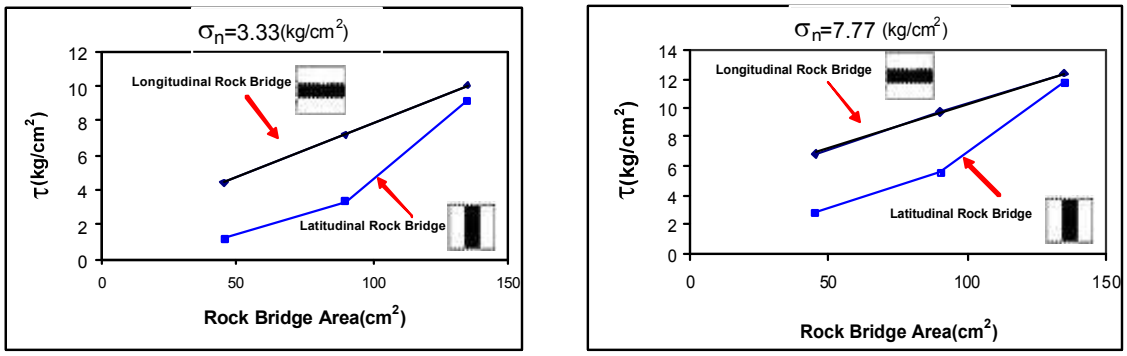

(a) (b)

Fig. 9: Shear resistance versus rock bridge area (for one latitudinal and longitudinal rock bridge); a: The normal stress is 3.33 kg cm^{-2}, b: The normal stress is 7.77 kg cm^{-2}

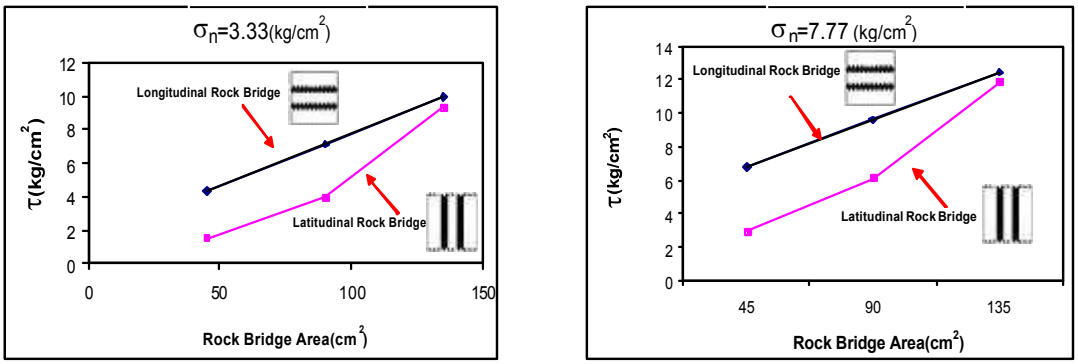

(a) (b)

Fig. 10: Shear resistance versus rock bridge area (for two latitudinal and longitudinal rock bridges); a: The normal stress is 3.33 kg cm^{-2}, b: The normal stress is 7.77 kg cm^{-2}

1: For the fixed area of the rock bridge under fixed normal stress the resistance of the latitudinal rock-bridges is less than the resistance of the longitudinal rock bridges (Fig. 9 and 10). Several aspects exist for this behavior:

When the rock-bridge surface occupies 45 cm^2 of the total shear surface: In this condition the EJC is zero for longitudinal rock-bridges (Table 2Aa and 2Ee) and the shear fracture occurred in rock segment (Fig. 4a and 4d) while for the latitudinal rock-bridges EJC is 0.8 (Table 2Bb and 2Ff) and tensile fracture takes place in the rock-bridge (Fig. 5a and 5d). Since the tensile resistance of the rock bridge is less than its shear resistance, hence the smaller external load needs to bring the latitudinal rock bridge to tensile failure.

When rock-bridge surface occupies 90 cm^2 of the total shear surface: In this condition the EJC is zero for longitudinal rock-bridges (Table 2Aa? and 2Ee?) and the shear fracture occurred in rock segment (Fig. 4b and 4e) while for the latitudinal rock-bridges EJC is 0.6 (Table 2Bb? and 2Ff?) and tensile fracture takes place in the rock-bridge (Fig. 5b and 5e). So similar to former case the smaller external load needs to bring the latitudinal rock bridge to tensile failure.

When rock-bridge surface occupies 135 cm^2 of the total shear surface: In this condition, the shear fracture is occurred in both longitudinal and latitudinal rock-bridges ((Fig. 4c and 4f) and (Fig. 5c and 5f)) but the shear resistance of the latitudinal rock-bridge is less than its amount in longitudinal rock bridges. This behavior could be attributed to another effective facture. So that the EJC is zero for longitudinal rock-bridges (Table 2Aa?? and 2Ee??) but for the latitudinal rock-bridges EJC=0.4 (Table 2Bb?? and 2Ff??). The more be EJC, the higher be stress concentration at tips of the joints. So the smaller external loading need for reaching the shear stress concentration at tips of the joints to critical value. It means that the shear resistance of the latitudinal rock-bridge is less than its amount in longitudinal rock bridges.

2: With the reduction of the rock-bridge area under the fixed normal stress, the resistance reduction rate for the

latitudinal rock-bridge is more than its amount for longitudinal rock-bridges (Fig. 9 and 10). This has several reasons:

2-1: for the longitudinal configuration of rock-bridges the joint surface does not exist in front of the rock-bridge and the reduction in rock-bridge area is the only factor for the resistance reduction. But for the latitudinal configuration of rock bridges the joint surfaces are presented in front of the rock-bridge. With the reduction of the rock bridge area, the joint surface is increased and the joint tips move closer to each other. Therefore a very high stress concentration (tensile and shear stress) is established at tip of the joints due to the interaction between the joint tips. These factors (i.e. the decreasing in rock bridge area and increasing in stress concentration) cause that the resistance reduction rate in the latitudinal rock-bridge be more than its amount in longitudinal rock-bridges.

2-2: With the reduction of the longitudinal rock-bridge area, the EJC=0 and the shear failure mode unchanged in the rock-bridge (Fig. 4). Therefore the shear resistance reduces at a linear rate. But for the latitudinal rock-bridge, with the reduction of the rock-bridge area, the EJC is increased and the shear failure mode changes to tensile failure (Fig. 5). Thus, the shear resistance reduces at a non-linear rate. It can be concluded from Fig, 9 and 10 that the EJC had significant effect on the resistance of rock bridge.

DETERMINATION OF THE SLIDE DIRECTION IN THE ROCK SLOPE WITH THE PRESENCE OF THE COPLANAR NON-PERSISTENT OPEN DISCONTINUITY

In the previous section, the effect of the effective joint Coefficient on the rock-bridge resistance is surveyed. In general, in the fixed area of the rock-bridge under fixed normal stress, the rock-bridge resistance is reduced with the increase of the Effective Joint Coefficient (EJC). With this experimental analysis, it is possible to determine the slide direction in the rock slopes containing coplanar non-persistent open discontinuity (Fig. 1). The openness of the joints and their engineering characteristics do not have any effect in the determination of the slide path. Also, it is assumed that the overburden weight W (normal stress) and the area of the rock-bridge have a same distribution in all of the possible slide paths and have no effect in the determination of slide path. In case, the effects of dynamic, water and asymmetrical forces are not considered, the configuration of the rock-bridges i.e. EJC lonely is the key factor in determination of the slide path. In this condition the slide takes place in the direction that has the maximum effective joint Coefficient (EJC). Because, the more be the maximum effective joint Coefficient, the less be the sliding surface resistance.

CONCLUSION

The shear behavior (failure progress, failure pattern, failure mechanism and shear resistance) of rock specimens containing various configurations of rock bridges with different areas has been investigated under two different normal loads through direct shear test. The results show that the failure pattern is mostly influenced by EJC (the ratio of the surface of the joint that is in front of the rock-bridge and the total shear surface) while shear resistance is closely related to failure pattern and its mechanism. The following conclusions can be drawn from the experimental tests:

1. In the fixed area of the rock-bridge under fixed normal stress, with the increase in the effective joint Coefficient, a very high stress concentration (tensile and shear stress) is established at tip of the joints due to the interaction between the joint tips.
2. With the increase in the effective joint Coefficient, the shear failure mode in the rock-bridge changes to the tensile failure mode.
3. The shear strength is closely related to the rock bridge failure pattern and failure mechanism, so that in the fixed area of the rock-bridge under fixed normal stress, the rock-bridge resistance reduced with change in failure mode from shear to tensile.
4. In the rock slopes containing coplanar non-persistent open discontinuity, assuming that the engineering characteristics of the joint, the overburden weight W (normal stress), the area of the rock-bridge, the dynamic, water and asymmetrical forces do not effect in the determination of the slide path, the slide will take place in the path which has the maximum amount of the effective joint coefficient. Because, the more be the maximum effective joint Coefficient, the less be the sliding surface resistance.

REFERENCES

1. Terzaghi, K., 1962. Stability of steep slopes on hard unweathered rock. Geotechnique, 12: 251-270.
2. Robertson, A.M., 1970. The interpretation of geological factors for use in slope theory. In: Planning Open Pit Mines, Proceedings, Johannesburg, pp: 55-71.

3. Einstein, H.H., D. Veneziano, G.B. Baecher and K.J. O'Reilly, 1983. The effect of discontinuity persistence on rock slope stability. Intl. J. Rock Mech. Min. Sci. Geomech. Abstr.l 20 (5): 227-236.
4. Jaeger, J.C., 1971. Friction of rocks and stability of rock slopes. Geotechnique, 21: 97-134.
5. Einstein, H.H., D. Veneziano, G.B. Baecher and K.J. O'Reillly, 1983. The effect of discontinuity persistence on rock slope stability. Intl. J. Rock Mech. Min. Sci. Geomech. Abstr., 20 (5): 227-236.
6. Lajtai, E.Z., 1969. Resistance of discontinuous rocks in direct shear. Geotechnique, 19: 218-233.
7. Reyes, O. and H.H. Einstein, 1991. Failure mechanisms of fractured rock-a fracture coalescence model. In: Proceedings of the Seventh International Congress Rock Mechanics, pp: 333-340.
8. Shen, B., O. Stephansson, H.H. Einstein and B. Ghahreman, 1996. Coalescence of fractures under shear stress experiments. J. Geophys. Res., 6: 5975-5990.
9. Bobet, A. and H.H. Einstein, 1998. Fracture coalescence in rock-type materials under uniaxial and biaxial compression. Intl. J. Rock Mech. Min. Sci., 35: 863-888.
10. Sagong, M. and A. Bobet, 2002. Coalescence of multiple flaws in a rock-model material in uniaxial compression. Intl. J. Rock Mech. Min. Sci., 39: 229-241.
11. Wong, R.H.C., KT. Chau, C.A. Tang and P. Lin, 2001. Analysis of crack coalescence in rock-like materials containing three flaws—Part I: experimental approach. Intl. J. Rock Mech. Min. Sci., 38: 909-924.
12. Mughieda, O.S. and I. Khawaldeh, 2006. Coalescence of offset rock joints under biaxial loading. Geotech. Geol. Eng., 24: 985-999.
13. Mughieda, O.S. and I. Khawaldeh, 2004. Scale effect on engineering properties of open non-persistent rock joints under uniaxial loading. KAYAMEK'2004-VII. Bölgesel Kaya Mekanigi Sempozyumu/ROCKMEC'2004-VIIth Regional Rock Mechanics Symposium, 2004, Sivas, Türkiye.
14. Li, Y.P., L.Z. Chen and Y.H. Wang, 2005. Experimental research on pre-Cracked marble. Intl. J. Solids Struct., 42: 2505-2016.
15. Shen, B., 1995. The mechanism of fracture coalescence in compression-experimental study and numerical simulation. Eng. Fracture Mech., 51 (1): 73-85.
16. Wong, R.H.C. and K.T. Chau, 1998. Crack coalescence in a rock-like material containing two cracks. Intl. J. Rock Mech. Min. Sci., 35 (2): 147-164.
17. Mughieda and A.K. Alzoubi, 2004. Fracture mechanisms of offset rock joints-A laboratory investigation. Geotech. Geol. Eng., 22: 545-562.
18. Gehle, C. and H.K. Kutter, 2003. Breakage and shear behavior of intermittent rock joints. Intl. J. Rock Mech. Min. Sci., 40: 687-700.
19. Ghazvinian, A., M.R. Nikudel and V. Sarfarazi, 2007. Effect of rock bridge continuity and area on shear behavior of joints. 11th congress of the international society for rock mechanics, Lisbon, Portugal.
20. Stimpson, B., 1970. Modeling materials for engineering rock mechanics. Intl. J. Rock Mech. Min. Sci. Geomech. Abstr., 7 (1): 77-121.
21. Nelson, R.A. and R.C. Hirschfeld, 1968. Modeling a jointed rock mass. Report R68-70, Mass. Inst. Technol., Cambridge.
22. Labuz, J.F., S.T. Dai and E. Papamichos, 1996. Plane-strain compression of rock-like materials. Intl. J. Rock Mech. Min. Sci. Geomech. Abstr., 33 (1): 573-584.
23. Momber, A.W. and R. Kovacevic, 1997. Test parameter analysis in abrasive water jet cutting of rocklike materials. Intl. J. Rock Mech. Min. Sci., 34 (1): 17-25.
24. Takeuchi, K., 1991. Mixed-mode fracture initiation in granular brittle materials. M.S. Thesis, Massachusetts Institute of Technology, Cambridge.
25. Shen, B., O. Stephansson, H.H. Einstein and B. Ghahreman, 1995. Coalescence of fractures under shear stress experiments. J. Geophy. Res., 100 (6): 5975-5990.
26. Nelson, R., 1968. Modeling a jointed rock mass. MS Thesis, Massachusetts Institute of Technology, Cambridge.
27. ASTM, 1986. Test method for unconfined compressive resistance of intact rock core specimens. ASTM designation D2938-86.
28. ASTM, 1971. Standard method of test for splitting tensile resistance of cylindrical concrete specimens. ASTM designation C496-71.
29. Stimpson, B., 1970. Modeling material for engineering rock mechanics. Intl. J. Rock Mech. Min. Sci., 7: 77-121.
30. Brown, E.T. and D.H. Trollop, 1970. Resistance of a model of jointed rock. In: J. Soil Mech. Found. Engrg, Proc. ASCE, 96: 685-704.

31. Rosenblade, J.L., 1971. Geomechanical model study of the failure modes of jointed rock masses, Ph.D Thesis, University of Illinois at Urbana-Champaign, Il, USA.
32. Ladanyi, B. and G. Archambault, 1980. Direct and indirect determination of shear resistance of rock mass. AIME Annual Meeting, Las Vegas. Preprint, pp: 80-25.
33. Zhang, H.Q., Z.Y. Zhao, C.A. Tang and L. Song, 2006. Numerical study of shear behavior of intermittent rock joints with different geometrical parameters. Intl. J. Rock Mech . Min. Sci., 43: 802-816.